Rapid Communications

Growth of a predicted two-dimensional topological insulator based on InBi-Si(111)-$\sqrt{7} \times \sqrt{7}$

Chia-Hsiu Hsu,[1] Zhi-Quan Huang,[2] Cho-Ying Lin,[3] Gennevieve M. Macam,[2] Yu-Zhang Huang,[3] Deng-Sung Lin,[3,*] Tai Chang Chiang,[4,5] Hsin Lin,[6,7,8,†] Feng-Chuan Chuang,[2,9,‡] and Li Huang[1,§]

[1]*Department of Physics, Southern University of Science and Technology, Shenzhen, Guangdong 518055, China*
[2]*Department of Physics, National Sun Yat-Sen University, Kaohsiung 804, Taiwan*
[3]*Department of Physics, National Tsing Hua University, Hsinchu 30013, Taiwan*
[4]*Department of Physics, University of Illinois, Urbana, Illinois 61801-3080, USA*
[5]*Frederick Seitz Materials Research Laboratory, University of Illinois, Urbana, Illinois 61801-2902, USA*
[6]*Institute of Physics, Academia Sinica, Taipei 11529, Taiwan*
[7]*Centre for Advanced 2D Materials and Graphene Research Centre, National University of Singapore, Singapore 117546*
[8]*Department of Physics, National University of Singapore, Singapore 117542*
[9]*Multidisciplinary and Data Science Research Center, National Sun Yat-Sen University, Kaohsiung 804, Taiwan*

(Received 21 January 2018; published 6 September 2018)

Using combined scanning tunneling microscopy (STM) measurements and first-principles electronic structure calculations, we extensively studied the atomic and electronic properties of a $\sqrt{7}$-InBi overlayer on Si(111). We propose and demonstrate an effective experimental process to successfully form a large well-ordered $\sqrt{7}$ surface by depositing Bi atoms on the In-Si(111)-4 × 1 substrate. The STM images exhibit a honeycomb pattern. After performing an exhaustive computational search, we identified the atomic structures of the surface at In and Bi coverages of 6/7 and 3/7 monolayers, respectively. We discovered a trimer model with a lower energy than the previously proposed model. The simulated STM images of trimer models confirm the presence of the honeycomb pattern in accord with our experimental STM images. Most importantly, we found that the surface is robust, preserving the topologically nontrivial phase. Our edge state calculations verify that the InBi overlayer on Si(111) is indeed a two-dimensional (2D) topological insulator (TI). Moreover, hybrid functional calculations result in band gaps up to 70 meV, which is high enough for room-temperature experiments. Our findings lay the foundation for the materials realization of 2D TIs by growing an InBi overlayer on a Si(111) substrate.

DOI: 10.1103/PhysRevB.98.121404

I. INTRODUCTION

Since their recent discovery, two-dimensional (2D) topological insulators (TIs) have become a subject of intensive research. These novel materials, also known as quantum spin Hall (QSH) insulators, surprisingly possess spin-polarized, gapless edge states with a Dirac-cone-like linear energy dispersion even though their interior is insulating [1–5]. Its versatile electronic properties make it a feasible material to integrate into the modern silicon industry. Furthermore, they are also potential candidate materials for low-energy consumption spintronics applications because their edge states are robust against nonmagnetic impurities. The existence of topological spin transport channels which was first demonstrated in an experiment is limited to quantum wells and measured at very low temperatures, despite the fact that the gaps could be up to 40 meV in theoretical predictions [6–8]. Thus, we are still challenged to search for new types of 2D TIs with band gaps large enough to support room-temperature applications.

QSH insulating phases have been discovered in numerous honeycomb materials [9–17]. Motivated by these discoveries and the experimental study of hydrogenated graphene [18], chemical functionalization such as hydrogenation and halogenation was utilized on honeycomb materials to explore for QSH phases [19–30]. Among them, numerous studies predicted potentially synthesized novel 2D TIs with band gaps large enough to exist at room temperature [12–16,23–28]. However, experimental realizations generally require a substrate to synthesize 2D TIs and also to ensure the predicted topological properties are achieved. Therefore, there is also a need to further understand the effects of the substrate on free-standing TIs.

A huge amount of effort and attempts have been made to realize substrate-supported 2D TIs [28–33]. A recent study predicted that planar honeycomb structures consisting of heavy metal elements, such as Bi with a large spin-orbit coupling (SOC), exist as TIs on SiC(0001) substrates [28]. This is because the bonding with the substrate leads to the removal of p_z bands in the Bi atom from the Fermi level and cause the system to induce a topological nontrivial phase. Later on, such a hexagonal honeycomb Bi was successfully grown on SiC(0001) [31] and confirmed the theoretical prediction [28]. Another type of system composed of surface alloys formed through Bi or In atom adsorption to construct a planar honeycomb on Au/Si(111) was also predicted as a 2D TI [32,33]. Unfortunately, the synthesized system is not

*dengsunglin@gmail.com
†nilnish@gmail.com
‡fchuang@mail.nsysu.edu.tw
§huangl@sustc.edu.cn

robust enough to maintain the nontrivial phase due to thermal buckling of the honeycomb [32,33].

Among the previously cited research on honeycomb structures, we highlight the study on a new class of III-V honeycombs [15], such as InBi and GaBi, which exhibit topological insulating phases. These 2D materials can hold the topological phase after hydrogenation and with a Si(111) substrate [26]. These systems lack sufficient research attention as there is a very limited number of reports on successful experiments [34–36]. Despite the difficulty, these type of surfaces are still deserving of in-depth explorations for their topological properties.

In this Rapid Communication, we improve the growth of a stable and ordered surface alloy, an InBi-$\sqrt{7} \times \sqrt{7}$ (hereafter referred to as $\sqrt{7}$) phase on a Si(111) substrate [34] and explore the atomic, electronic, and topological properties of this system. Our experimental result shows that the $\sqrt{7}$ reconstruction is a stable state and is effectively achieved by depositing Bi on In-Si(111)-4 × 1. Using first-principles electronic structure calculations and scanning tunneling microscopy (STM), we systematically examine the atomic structures of the $\sqrt{7}$ phase [34]. We find our trimer model to have a lower energy than the previously proposed one [34]. The STM measurement reveals the formation of a hexagonal pattern, which is consistent with our theoretical structural calculations. Most significantly, these two low-energy lying trimer models (denoted as T1-T4 and T1-H3 models) are identified as topologically nontrivial materials. Heyd-Scuseria-Ernzerhof (HSE06) [37] calculations reveal that the band gap is as large as 70 meV for a T1-T4 model. The orbital analysis of the electronic structure shows that the surface bands near the Fermi level were composed of s-orbital In atoms and p_x and p_y orbitals of both In and Bi atoms. Finally, we theoretically demonstrate the edge state of a semi-infinite InBi-Si(111)-$\sqrt{7}$ ribbon to validate its topological properties.

II. METHODS

The STM measurements were carried out in an ultrahigh vacuum (UHV) chamber with a base pressure below 2.0×10^{-10} Torr. The Si(111) substrate was cut from a silicon wafer with a size of 2×10 mm^2. After 12 h of outgassing at about 800 K, an atomically clean Si(111) surface was obtained by direct-current heating to ∼1450 K for a few seconds. The indium and bismuth atomic beams were generated by e-beam evaporators located about 7 cm away from the Si(111) substrate. The deposition rates are ∼0.17 ML/min, where 1.0 monolayer (ML) is 7.84×10^{14} atoms/cm^2 for Si(111).

The first-principles calculations were performed within the density functional theory framework [38] using the generalized gradient approximation [39] and projector augmented-wave potentials [40], as implemented in the Vienna *ab initio* simulation package [41]. The kinetic energy cutoff was set at 400 eV. The system was simulated using a periodically repeating slab which consists of four Si bilayers, a reconstructed layer, and a vacuum space of ∼20 Å. The Si dangling bonds at the bottom of the slab were passivated using hydrogen atoms. The lattice constant of the lowermost Si bilayer was set to the theoretical value of 5.468 Å and the atoms situated

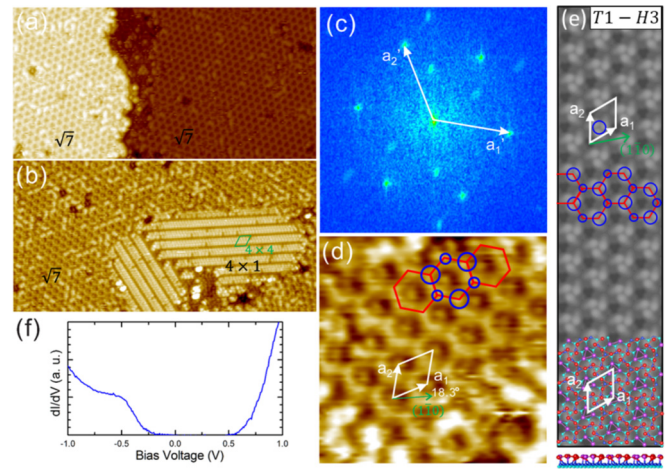

FIG. 1. Filled state STM images of the Si(111) surface after (a) the deposition of 0.4-ML Bi on the In-Si(111)-4 × 1 surface and (b) codeposition of 1.2-ML Bi and 0.9-ML In at RT and subsequent annealing at 770 K. $V_s = -1.1$ V; $I_t = 0.20$ nA; size: 40×20 nm^2. The small thermal drift in the images is not corrected. In (b), the surface consists mainly of $\sqrt{7}$ domains and some 4 × 1 areas. (c) Fourier transform of (b). (d) 6×6 nm^2 zoomed-in STM image of the upper left area in (b). The white solid arrows in (c) point to first-order diffraction spots corresponding to the unit cell vectors in (d). (e) Simulated STM image of the T1-H3 trimer model. The white line denotes a $\sqrt{7}$ unit cell in (d). (f) STS spectrum taken in a $\sqrt{7}$ area.

here were not optimized. The remaining Si, In, and Bi atoms were relaxed using the conjugate gradient method until the residual force on each atom was smaller than 0.001 eV/Å. The surface Brillouin zones (SBZs) of the $\sqrt{7}$ phases were sampled using a Γ-centered $6 \times 6 \times 1$ Monkhorst-Pack [42] grid. SOC was included for all the band-structure calculations. The topology of the band structures was identified according to the method of Ref. [43] for calculating the Z_2 invariant in terms of the so-called n-field configuration of the system. The edge states were calculated from the Green's function of the semi-infinite model [44,45] with the Hamiltonian derived from maximally localized Wannier functions obtained via the WANNIER90 package [46].

III. RESULTS AND DISCUSSION

In our experiment, a two-step approach was employed to grow a full $\sqrt{7}$-InBi layer. First, an In-Si(111)-4 × 1 surface was prepared by depositing 1.0-ML In on Si(111)-7 × 7 at room temperature (RT), followed by annealing at 730 K for 60 s [47]. The second step was to deposit 0.4-ML Bi on the In-Si(111)-4 × 1 surface at RT, and subsequently anneal at 730 K for 60 s. This two-step approach can produce the $\sqrt{7}$-InBi phase that covers nearly the entire surface of the substrate, as shown in Fig. 1(a). The theoretically proposed model for the $\sqrt{7}$-(In,Bi) structure contains ∼0.86 ML of In and ∼0.43 ML of Bi [34]. Our intensity analysis of synchrotron-radiation core-level photoemission (not shown here) for a similarly prepared surface shows that the In coverage is ∼0.8 ML and that of Bi is ∼0.4 ML. Apparently, indium atoms were partially desorbed during the annealing process.

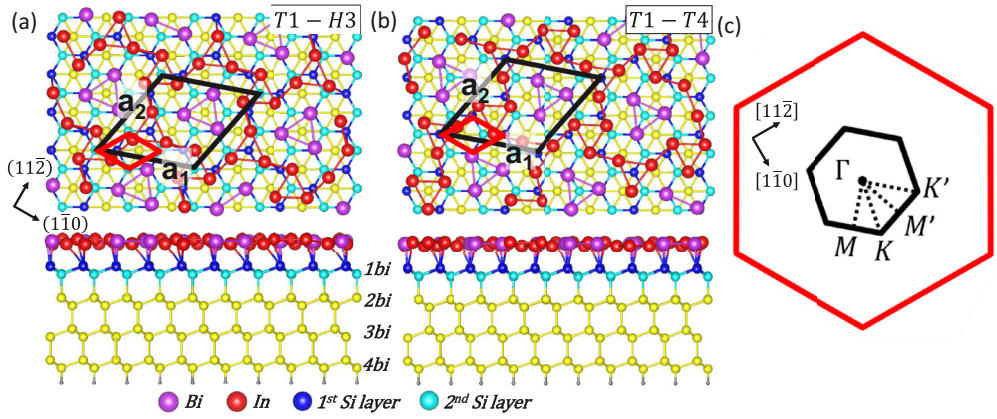

FIG. 2. Top and side views of the structural models, (a) T1-H3 and (b) T1-T4, of InBi-Si(111)-$\sqrt{7}$. The black and red line marks the unit cell of the $\sqrt{7} \times \sqrt{7}$ and 1×1 phases, respectively. The 2D Brillouin zone (BZ) with specific symmetry points labeled is shown in (c). The BZs of $\sqrt{7} \times \sqrt{7}$ and 1×1 are indicated by black and red lines, respectively.

In order to include an internal lattice reference from the substrate to build the $\sqrt{7}$ structure model, we have also grown a layer that consists of both the $\sqrt{7}$-InBi and the 4×1-In domains, as displayed in Fig. 1(b). The mixed-phase surface is obtained by codeposition of 1.15-ML Bi and 0.86-ML In at RT and subsequent annealing at 770 K. The atomic arrangement of the $\sqrt{7}$ structure clearly exhibits a honeycomb structure, similar to that found in a previous report [34]. The corresponding Fourier transform image shown in Fig. 1(c) confirms the $\sqrt{7}$ periodicity. The lattice constant is $\sim 1.02 \pm 0.03$ nm, which is in good agreement with the $\sqrt{7}$ periodicity (1.016 nm). In Fig. 1(d), an obvious hexagonal shape (outlined by blue circles and red lines) is observed. The angle between the $\sqrt{7}$ and [1$\bar{1}$0] measures as 18.3°, close to the ideal value of 19.1°. In addition, the scanning tunneling spectroscopy (STS) measurements of the $\sqrt{7}$ structure [Fig. 1(f)] are also consistent with the previous experimental study [34].

The $\sqrt{7}$ phase of the InBi overlayer on Si(111) is composed of three Bi atoms and six In atoms. The previously proposed trimer model [34] defines a Bi trimer as a structure composed of three Bi atoms, as shown in Fig. 2(b). The Bi trimers can be labeled based on their location, i.e., the positions of the three Bi atoms and the Bi trimer center. Hence, we identify the previously proposed trimer model as a T1-T4 model in Fig. 2(b). The labels T1 and T4 correspond to sites above the top and second layer of the first bilayer of the underlying Si(111) substrate, respectively. Moreover, we have also later considered the H3 site which is above the top position of the second bilayer of Si(111). To conduct an exhaustive structural search, we considered different possible combinations of the Bi atoms and Bi trimer center locations. Six structural models are generated by considering any two sites of T1, T4, and H3 sites. In addition, we also performed a random search by positioning three Bi atoms arbitrarily at any three positions from nine atomic sites on the alloy surface of the T1-T4 model and filled the rest with In atoms. In this way, we are able to generate 84 initial structures for relaxations. These two methods yielded a total of 90 initial structures for optimization using the conjugate gradient method. After our systematic search, two kinds of low-energy structural models were found and summarized, namely, the line model and trimer model. As expected, we found the structures from the previously proposed T1-T4 model [34], and also identified a different trimer model, the T1-H3 (i.e., Bi atoms on T1 sites and Bi trimers on H3 sites) model, which has a lower energy of 21 meV. The top and side views of this low-energy lying T1-H3 model are shown in Fig. 2(a). In contrast with the old T1-T4 model, the Bi atoms of this T1-H3 model are likewise placed on T1 sites but the centers of the trimers are shifted from T4 to H3 sites. Other low-energy lying models are labeled as the line models (labeled as LM-1 and LM-2) presented in Supplemental Fig. S1 [48].

To determine the atomic structure, simulated STM images of the aforementioned four models are shown in Supplemental Fig. S2 [48]. Only the simulated STM images of trimer models exhibit the honeycomb pattern. The simulated STM image of the T1-H3 model with a sample bias of -1.0 eV shown in Fig. 1(e) has one brighter point in a unit cell. An obvious hexagonal shape (blue circles and red lines) consistent with the experimental results was observed. The adjacent indium trimers formed major and minor bright areas, indicated by large and small blue circles, respectively. For the rest of the discussion, we will focus on the trimer models.

After determining the atomic structures, we now proceed to the electronic properties of the $\sqrt{7}$ phase. The band structures of the two trimer models, T1-H3 and T1-T4, are shown in Figs. 3(a) and 3(b), respectively. The red lines denote the valence band maximum of the system. The band structures of these two trimer models are quite similar, we observe semimetallic properties in both models but the band dispersions occur at different paths, since $\sqrt{7}$ has a threefold symmetry. Next, we analyzed the orbital contributions of the T1-H3 trimer model as presented in Figs. 3(c)–3(e) because this model has a lower energy and is consistent with the STM images. We found that the main contribution of surface states near the Fermi level was from the p_x, p_y orbitals of the Bi atom and s, p_x, p_y orbitals of the In atoms as well as Si-p_z of the first Si bilayer. The valence band S_1 was composed of In-s and Si-p_z orbitals which indicate that an s-p_z bond was formed. Here, S_1 represents a pair of splitting bands with a similar energy dispersion. The S_2 was contributed from the In-s and Bi-p_x and Bi-p_y. The conduction bands S_3 and S_4

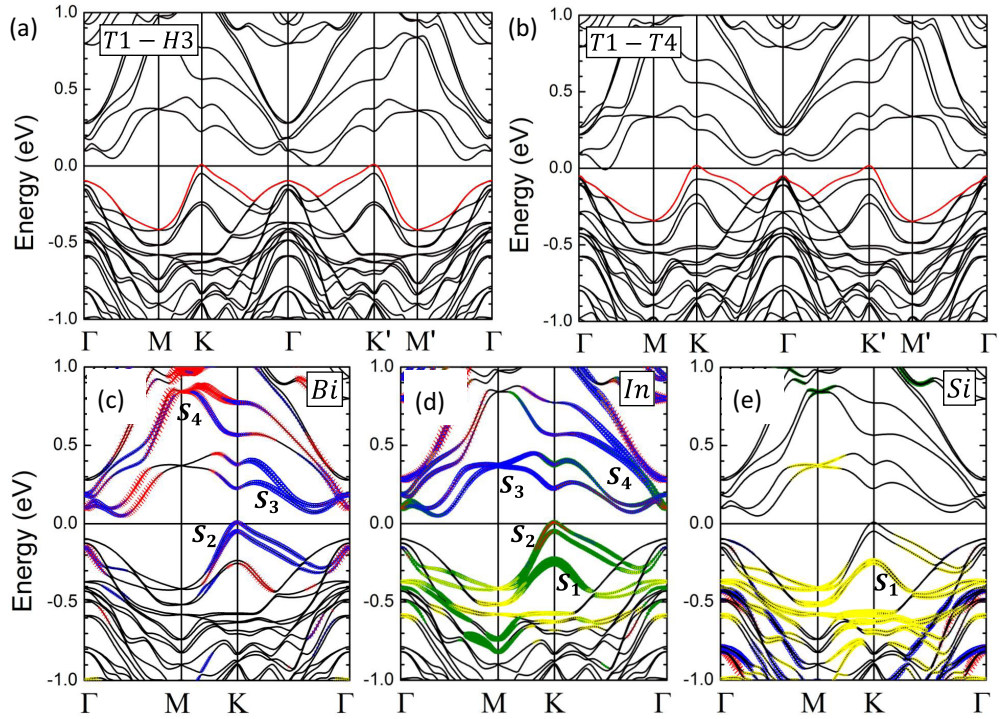

FIG. 3. Band structures of (a) T1-H3 and (b) T1-T4 trimer models. The valence band maximum is indicated by a red line. (c)–(e) are the band structures of Bi, In, and the first bilayer of the Si substrate, respectively, of the T1-H3 trimer model. The olive circles, red crosses, blue circles, and yellow circles, respectively, denote the s-, p_x-, p_y-, and p_z-orbital contributions.

were both composed of the p_x and p_y orbitals of In and Bi atoms but S_3 also includes In-s orbitals.

Since two trimer models (T1-H3 and T1-T4) and one line model (LM-2) are semimetallic, we further calculated the Z_2 topological invariant. The results of Z_2 calculations are shown in Supplemental Fig. S3 [48]. Interestingly, we found three models harboring topological nontrivial phases with $Z_2 = 1$, implying the robustness of the topological phase.

An additional analysis using hybrid functional HSE06 calculations was used to correct the underestimated system band gap. Since HSE06 calculations require more computational resources, we would like to reduce the thickness of the Si substrate as much as possible. Therefore, before further calculations, we are interested in the change of electronic structure when decreasing the number of bilayers (BLs) on the Si(111) substrate. Supplemental Fig. S4 shows the band structure of the T1-H3 model with the substrate constructed from one to four Si BLs [48]. We found that the features of the system remain a semimetal with the nontrivial topological phase ($Z_2 = 1$), but the gap and a few bands near the Fermi level show a slight change with the number of bilayers. For the purposes of reducing computational time and resources, two Si BLs were employed as the substrate for the HSE06 calculations. The band structures of two trimer models with different functionals, Perdew-Burke-Ernzerhof (PBE) and HSE06, are shown in Figs. 4(a) and 4(b) for T1-H3 and T1-T4, respectively. The band gap of the T1-T4 model increased to 70 meV after HSE06 calculations. Due to the localization of the STS measurement, the experimental results are mainly dominated by the contribution of the Γ point in momentum (reciprocal) space. Therefore, we found that the gap at the Γ point is 330 (387) meV for the T1-T4

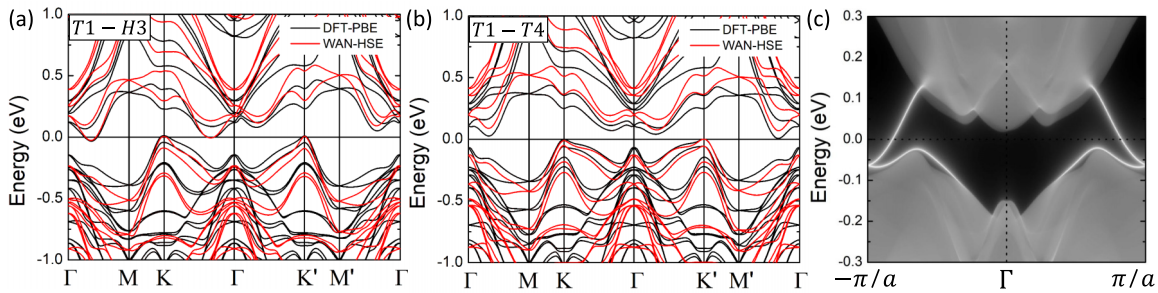

FIG. 4. Band structures using PBE and hybrid functional (HSE06) including SOC calculations for the (a) T1-H3 model and (b) T1-T4 model, respectively. Two Si BLs are used for the substrate. (c) is the edge band structure of the T1-T4 model.

(T1-H3) model, which is close to the experimental results of ∼500 meV.

We gain further insight into the nontrivial band topologies resulting from an adsorbed In-Bi overlayer on Si(111)-$\sqrt{7}$ by carrying out edge state calculations. Here, we examine the T1-H4 model. A two-bilayer Si(111) substrate was used for the edge state calculation. Based on the results of the HSE06 calculation, the Green's function of the semi-infinite model was constructed to calculate the local density of states of the edge, as shown in Fig. 4(c). The brighter (white) bands resulting from the edge connected the valence and conduction bands within the bulk gap. In particular, for each edge, an even number of edge states are seen to cross the Fermi level between two high symmetry points, Γ and π/a in Fig. 4(c), confirming that the system is indeed a 2D TI.

IV. CONCLUSIONS

In summary, we have grown and identified 2D Tls based on an InBi overlayer on Si(111)-$\sqrt{7}$ by using STM measurements and first-principles electronic structure calculations. We demonstrated the formation of a well-ordered $\sqrt{7}$ reconstruction which can be attained by the deposition of Bi on an In-Si(111)-4 × 1 substrate. We have systematically examined the atomic structures of the $\sqrt{7}$ phase and found the trimer T1-H3 model which has a lower energy of 21 meV than the previously proposed T1-T4 model. Our STM experiment confirmed the presence of a honeycomb pattern in the InBi overlayer on Si(111)-$\sqrt{7}$ which matches our theoretical structure predictions. The topological nontrivial phase has been confirmed by calculating the Z_2 invariant and a set of edge states which connected the valence and conduction bands. The HSE06 calculations reveal that the band gap is up to 70 meV for trimer models. Our findings show that InBi-Si(111)-$\sqrt{7}$ can provide a viable platform for hosting 2D topological phases, including the possibility of tuning the topological state via gating (out-of-plane electric field) [12] and/or further doping of the surface.

ACKNOWLEDGMENTS

C.H. and L.H. acknowledge the support by the NSFC under Grants No. 11704176, No. 11404160, and No. 11774142, and Shenzhen Peacock Plan Team under Grant No. KQTD2016022619565991. F.C.C. acknowledges support from the National Center for Theoretical Sciences and the Ministry of Science and Technology of Taiwan under Grant No. MOST-104-2112-M-110-002-MY3 and the support under NSYSU-NKMU joint research Projects No. 105-P005 and No. 106-P005. He is also grateful to the National Center for High-Performance Computing for computer time and facilities. D.S.L. acknowledges the financial support from the Ministry of Science and Technology of Taiwan under Grant No. MOST-105-2112-M-007-018. H.L. acknowledges the Singapore National Research Foundation for support under NRF Award No. NRF-NRFF2013-03. T.C.C. acknowledges support from the US National Science Foundation under Grant No. DMR-17-09945.

C.-H.H., Z.-Q.H., and C.-Y.L. are contributed equally to this work.

[1] A. Bansil, H. Lin, and T. Das, Rev. Mod. Phys. **88**, 021004 (2016).
[2] C. L. Kane and E. J. Mele, Phys. Rev. Lett. **95**, 146802 (2005).
[3] X. L. Qi, T. L. Hughes, and S. C. Zhang, Phys. Rev. B **78**, 195424 (2008).
[4] M. Z. Hasan and C. L. Kane, Rev. Mod. Phys. **82**, 3045 (2010).
[5] X.-L. Qi and S.-C. Zhang, Rev. Mod. Phys. **83**, 1057 (2011).
[6] B. A. Bernevig, T. L. Hughes, and S.-C. Zhang, Science **314**, 1757 (2006).
[7] M. König, S. Wiedmann, C. Brüne, A. Roth, H. Buhmann, L. W. Molenkamp, X.-L. Qi, and S.-C. Zhang, Science **318**, 766 (2007).
[8] A. Roth, C. Brüne, H. Buhmann, L. W. Molenkamp, J. Maciejko, X.-L. Qi, and S.-C. Zhang, Science **325**, 294 (2009).
[9] W.-F. Tsai, C.-Y. Huang, T.-R. Chang, H. Lin, H.-T. Jeng, and A. Bansil, Nat. Commun. **4**, 1500 (2013).
[10] C.-C. Liu, W. Feng, and Y. Yao, Phys. Rev. Lett. **107**, 076802 (2011).
[11] Z.-Q. Huang, C.-H. Hsu, F.-C. Chuang, Y.-T. Liu, H. Lin, W.-S. Su, V. Ozoliņš, and A. Bansil, New J. Phys. **16**, 105018 (2014).
[12] F.-C. Chuang, C.-H. Hsu, C.-Y. Chen, Z.-Q. Huang, V. Ozoliņš, H. Lin, and A. Bansil, Appl. Phys. Lett. **102**, 022424 (2013).
[13] Y. Xu, B. Yan, H.-J. Zhang, J. Wang, G. Xu, P. Tang, W. Duan, and S.-C. Zhang, Phys. Rev. Lett. **111**, 136804 (2013).
[14] M. Wada, S. Murakami, F. Freimuth, and G. Bihlmayer, Phys. Rev. B **83**, 121310 (2011).
[15] F.-C. Chuang, L.-Z. Yao, Z.-Q. Huang, Y.-T. Liu, C.-H. Hsu, T. Das, H. Lin, and A. Bansil, Nano Lett. **14**, 2505 (2014).
[16] Z.-Q. Huang, F.-C. Chuang, C.-H. Hsu, Y.-T. Liu, H.-R. Chang, H. Lin, and A. Bansil, Phys. Rev. B **88**, 165301 (2013).
[17] C. L. Kane and E. J. Mele, Phys. Rev. Lett. **95**, 226801 (2005).
[18] D. C. Elias, R. R. Nair, T. M. G. Mohiuddin, S. V. Morozov, P. Blake, M. P. Halsall, A. C. Ferrari, D. W. Boukhvalov, M. I. Katsnelson, A. K. Geim *et al.*, Science **323**, 610 (2009).
[19] J. O. Sofo, A. S. Chaudhari, and G. D. Barber, Phys. Rev. B **75**, 153401 (2007).
[20] J. C. Garcia, D. B. de Lima, L. V. C. Assali, and J. F. Justo, J. Phys. Chem. C **115**, 13242 (2011).
[21] C. H. Zhang and S. S. Yan, J. Phys. Chem. C **116**, 4163 (2012).
[22] R. Wang, S. Wang, and X. Wu, J. Appl. Phys. **116**, 024303 (2014).
[23] B.-H. Chou, Z.-Q. Huang, C.-H. Hsu, F.-C. Chuang, Y.-T. Liu, H. Lin, and A. Bansil, New J. Phys. **16**, 115008 (2014).
[24] C.-C. Liu, S. Guan, Z. Song, S. A. Yang, J. Yang, and Y. Yao, Phys. Rev. B **90**, 085431 (2014).
[25] Z. Song, C.-C. Liu, J. Yang, J. Han, M. Ye, B. Fu, Y. Yang, Q. Niu, J. Lu, and Y. Yao, NPG Asia Mater. **6**, e147 (2014).
[26] C. P. Crisostomo, L.-Z. Yao, Z.-Q. Huang, C.-H. Hsu, F.-C. Chuang, H. Lin, M. A. Albao, and A. Bansil, Nano Lett. **15**, 6568 (2015).

[27] L.-Z. Yao, C. P. Crisostomo, C.-C. Yeh, S.-M. Lai, Z.-Q. Huang, C.-H. Hsu, F.-C. Chuang, H. Lin, and A. Bansil, Sci. Rep. **5**, 15463 (2015).
[28] C.-H. Hsu, Z.-Q. Huang, F.-C. Chuang, C.-C. Kuo, Y.-T. Liu, H. Lin, and A. Bansil, New J. Phys. **17**, 025005 (2015).
[29] M. Zhou, W.-M. Ming, Z. Liu, Z.-F. Wang, Y.-G. Yao, and F. Liu, Sci. Rep. **4**, 7102 (2014).
[30] M. Zhou, W. Ming, Z. Liu, Z.-F. Wang, P. Li, and F. Liu, Proc. Natl. Acad. Sci. USA **111**, 14378 (2014).
[31] F. Reis, G. Li, L. Dudy, M. Bauernfeind, S. Glass, W. Hanke, R. Thomale, J. Schäfer, and R. Claessen, Science **357**, 287 (2017).
[32] B. Huang, K.-H. Jin, H. L. Zhuang, L. Zhang, and F. Liu, Phys. Rev. B **93**, 115117 (2016).
[33] F.-C. Chuang, C.-H. Hsu, H.-L. Chou, C. P. Crisostomo, Z.-Q. Huang, S.-Y. Wu, C.-C. Kuo, W.-C. V. Yeh, H. Lin, and A. Bansil, Phys. Rev. B **93**, 035429 (2016).
[34] N. V. Denisov, A. A. Alekseev, O. A. Utas, S. G. Azatyan, A. V. Zotov, and A. A. Saranin, Surf. Sci. **651**, 105 (2016).
[35] D. V. Gruznev, L. V. Bondarenko, A. V. Matetskiy, A. N. Mihalyuk, A. Y. Tupchaya, O. A. Utas, S. V. Eremeev, C.-R. Hsing, J.-P. Chou, C.-M. Wei, A. V. Zotov, and A. A. Saranin, Sci. Rep. **6**, 19446 (2016).
[36] N. V. Denisov, A. A. Alekseev, O. A. Utas, S. G. Azatyan, A. V. Zotov, and A. A. Saranin, Surf. Sci. **666**, 64 (2017).
[37] A. V. Krukau, O. A. Vydrov, A. F. Izmaylov, and G. E. Scuseria, J. Chem. Phys. **125**, 224106 (2006).
[38] P. Hohenberg and W. Kohn, Phys. Rev. **136**, B864 (1964); W. Kohn and L. J. Sham, *ibid.* **140**, A1133 (1965).
[39] J. P. Perdew, K. Burke, and M. Ernzerhof, Phys. Rev. Lett. **77**, 3865 (1996).
[40] G. Kresse and D. Joubert, Phys. Rev. B **59**, 1758 (1999).
[41] G. Kresse and J. Hafner, Phys. Rev. B **47**, 558 (1993); G. Kresse and J. Furthmüller, *ibid.* **54**, 11169 (1996).
[42] H. J. Monkhorst and J. D. Pack, Phys. Rev. B **13**, 5188 (1976).
[43] T. Fukui and Y. Hatsugai, J. Phys. Soc. Jpn. **76**, 053702 (2007).
[44] M. P. L. Sancho, J. M. L. Sancho, and J. Rubio, J. Phys. F **15**, 851 (1985).
[45] Q.-S. Wu, S.-N. Zhang, H.-F. Song, M. Troyer, and A. A. Soluyanov, Comput. Phys. Commun. **224**, 405 (2018).
[46] A. A. Mostofi, J. R. Yates, Y.-S. Lee, I. Souza, D. Vanderbilt, and N. Marzari, Comput. Phys. Commun. **178**, 685 (2008).
[47] G. Lee, S.-Y. Yu, H. Kim, J.-Y. Koo, H.-T. Lee, and D. W. Moon, Phys. Rev. B **67**, 035327 (2003).
[48] See Supplemental Material at http://link.aps.org/supplemental/10.1103/PhysRevB.98.121404 for details on the atomic and band structures of the line models, simulated STM images of the discussed models, the band structures of different thicknesses of the Si substrate, and the calculation of the Z_2 invariant.